International Journal of Theoretical and Applied Research (IJTAR)
ISSN: 2812-5878

Homepage: https://ijtar.journals.ekb.eg

Original article

Comparative Electrochemical Studies of Niobium, Molybdenum, Cobalt Chromium Alloy and Gold Electrodes in Milk and Tap Water

F.M. Abou Koffa[a], E. M. Attia[b,*] and R.M. Abou Shahba[b]

[a] *Additives and Miscellaneous Department at Central Public Health Laboratories - Ministry of Health*
[b] *Chemistry Department, Faculty of Science (Girls), Al-Azhar University, Nasr City, Cairo, Egypt*

ARTICLE INFO

Received 01/04/2023
Revised 30/12/2023
Accepted 14/01/2024

Keywords

Dental electrodes
Tap water
Milk
Open circuit
Potentiodynamic polarization

ABSTRACT

In both milk and water, the corrosion behavior of four distinct electrodes—niobium, molybdenum, cobalt chromium-alloy, and gold electrodes—was studied at temperatures ranging from 20 to 50°C. Analysis of tap water and milk was performed. Open circuit potential and potentiodynamic polarization experiments were used in the inquiry. The open circuit data show the four electrodes' declining steady potential values (E_{ss}) in the ensuing direction: CoCr- Alloy > Au > Mo > Nb. For water and milk, this sequence was followed regardless of temperature. But milk at 50°C modified the order to be: Au > CoCr- alloy > Mo > Nb. At all temperatures, the E_{ss} values in tap water were higher than those in milk solutions, indicating more passivation in tap water. All of the investigated electrodes show rising corrosion rate (C_R) values during potentiodynamic polarization experiments as the solution temperature rises. At all temperatures, milk had greater C_R values than tap water for the four electrodes. According to C_R values, the following is the order of passivity: Au > Mo > CoCr-alloy > Nb in milk, Au > Mo > Nb > CoCr- alloy in water. Calculations and discussions were made about the activation energy (E_a), enthalpy change (ΔH°), and entropy change (ΔS°) of corrosion.

Graphical abstract

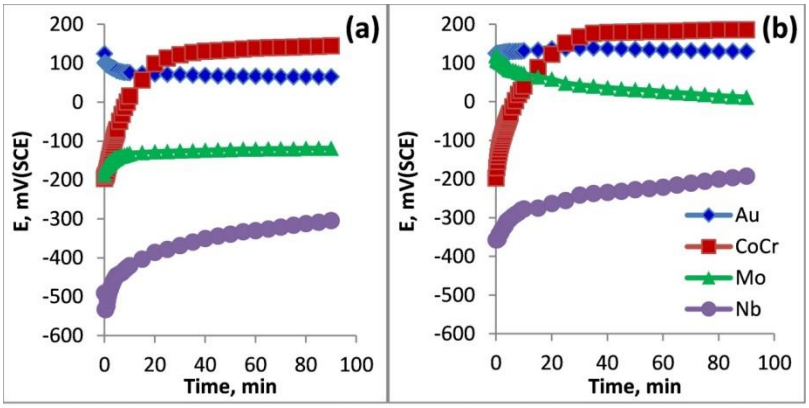

Potential – time plots of the studied electrodes in milk (a) and water (b) at 30 °C.

1. Introduction

Since gold is a noble metal that doesn't react with either air or water, it is frequently utilized in dental practice. The performance of prosthetic restorations created from gold using the conventional casting procedure is superior to those made from non-noble metals [1]. According to the Pourbaix diagram [2], niobium is very reactive with water and has a high chance of reaction, which indicates the production of a passive surface oxide film that gives it the appearance of being inert. The

* *Corresponding author*
E-mail address: Attiaenas.5919@azhar.edu.eg

DOI: 10.21608/IJTAR.2024.168826.1011

Special issue "selected papers from the 2nd International Conference on Basic and Applied Science (2nd IACBAS-2023)"

stable niobium pentoxide in this film is what gives the metal its biocompatibility. When the metal is in contact with oxygen, it forms rapidly and spontaneously [3]. In addition, Nb is used to create dental alloys because it is a β-stabilizing alloying element [4–8]. Due to its high melting point and tensile strength, molybdenum has the potential to be a highly creep-fatigue-resistant metal [9]. Due to the oxide's compact and flawless structure, it forms a highly stable oxide film in aqueous solutions [10, 11]. Mo's high tensile strength values allow for stents to have thinner struts, which improves flexibility and allows for access to vessels with narrower bores [12]. Because of their affordable price, excellent qualities, and increased resistance to distortion at high temperatures, basic metal alloys are frequently employed in dentistry [13]. The Cobalt-Chromium (CoCr-) alloys are a well-known illustration of base-metal alloys. They have numerous biomedical uses in the dentistry and orthopedic industries. [14-16]. The primary component of milk, which contains both major and minor salts, is water. The main salts include sodium, calcium, and magnesium chlorides, phosphates, and citrates. The solubility of the salts is influenced by temperature, humidity, and pH changes. The introduction of various elements such as copper, iron, nickel, and zinc to milk can be done by the use of equipment and food [17, 18]. On the other hand, environmental factors, such as the animal's breed, lactation stage, age, and health state, have an impact on the milk's ingredients. This study used Niobium, Molybdenum, and Cobalt Chromium-alloy electrodes that were evaluated in water and milk to examine the viability of utilizing gold substitutes in dental applications. At various temperatures ranging from 20 to 50°C, potentiodynamic polarization and open circuit potential approaches were used.

2. Material and methods

2.1. Preparation of electrodes

Working electrodes included 0.196 cm² of molybdenum rod provided by Aldrich-Chemie and 0.33 cm² of cylindrical pure niobium brought by Johnson Matthey- England. A second CoCr-alloy electrode in which Co was the main constituent, with Cr and Mo as the primary alloying elements has a surface area of 1.038 cm² with a composition of 64% Cobalt, 28% Chromium, 6% Molybdenum, and 2% (Carbon + Silicon + Manganese) was also employed. As a blank electrode, a golden rod with a surface area of 0.0184 cm², 98.2% Au, 1.7% Ti, and 0.1% Ir was employed. Using epoxy glue Araldite, each electrode was placed into a hollow glass cylinder of the proper diameter, leaving only the surface area in contact with the electrolyte. The electrode surfaces were polished with emery papers of increasing grit. Bi-distilled water was used to wash the electrodes to get rid of the slick particles. The electrodes' surfaces were then polished once more with a soft cloth before being completely submerged in the test solution.

2.2. Solution

Tap water and milk were used as the testing solutions. The milk was used without dilution and the packed used was ultra-high temperature processing (UHT) milk from cow milk (3% fat, 8.5% SNF) free from preservatives by the Egyptian Company for Dairy Products (Juhayna). The packing materials of the samples were cardboard paper.

2.3. Experimental techniques

2.3.1. Tap water and milk analysis

All analyses of tap water and milk were performed in the Ministry of Health and Population, preventive sector, Central Health Laboratory, Egypt. The physical analyses for tap water were done using a corporater (for residual chlorine), Turbidity meter, pH and Conductivity meter. Chemical analyses were performed using Flame Photometer, Ion Chromatography, and UV Vis Spectrophotometer Double Beam analyzer, in addition to normal titration tests. The recorded pHs were 6.6 and 7.5 for milk and tap water respectively.

The analyses of milk were performed using Milcoscan FT3-IR. Chemical-preservative analyses for sorbic and benzoic acids and their salts were performed using HPLC-thermo. Heavy metal chemical analysis was performed using Atomic Absorption.

2.3.2. Measurements of the open circuit potential (OCP)

In this method, measurements were performed in a glass cell that could hold 25 ml solution. The potential readings were obtained using a saturated calomel electrode (SCE) as a reference electrode and a digital multimeter (KEITHLEY, Model 175, USA).

2.3.3. Measurements of the Potentiodynamic polarization

An Electronic Potentioscan Wenking (Model POS 73) was used to measure potentiodynamic polarization. The measurements were made utilizing a platinum sheet as a supporting electrode and a saturated calomel electrode (SCE). The four electrodes were subjected to a scan rate of 3.33 mV/s starting at -5 up to +5 V/SCE to accomplish the polarization, and the resulting currents were recorded. To get the stabilized OCP value, the measurements were performed after dipping the electrodes for 90 min in the test solution.

3. Results and discussion

3.1. Tap water and milk analysis

Tap water was submitted to different types of analyses such as physical, chemical, and heavy metal chemical analysis. Add to these, microscopic- biological and microbiological analysis. Physical, chemical and heavy metal analyses were the only concerned in this study. The reference available range were subjugated to decision 458- 2007.

Six different samples of tap water were subjected to different analyses. Three of which are taken in the same day, on 26 of October, 2023 at different time intervals. The collected analytical data were recorded in Table 1. Another three different samples were taken among three months in 2023. The samples symbolized as 1, 2 and 3 were taken on the day 20 of August, 10 of September and 15 of October, respectively. The collected analytical data are recorded in Table 2. Tables 1 and 2 illustrate that the different elements and chemical compounds present in tap water cannot be quantified by a fixed amount for all samples. It is clear from the analyses that each water sample has its own characteristics and cannot in any way coincide with another sample.

The analysis of milk get down to human health was concerned with microbiology (not included in this research), chemical and chemical-preservatives analyses which take the numbers from 1 to 8 in Table 3. These chemical analyses were subjugated to the available reference range according to Egyptian Specification 1623-2005. Vessel-heavy metal chemical analysis (detection of lead) and toxicological fungous were subjugated to Egyptian specifications 7136-2010 and 7136-2020 respectively. The chemical analyses illustrated the narrow difference in the percentage values concerned with fats, solids …etc. as illustrated in Table 3. These approximate values were attributed to the same treatment furnished by the company (Juhayna) to produce its milk product. Get down to milk analysis, Mohamed *et al* [19] are concerned with the limited concentration (for human uses) of some heavy metals such as Pb, Cd, Cu, Zn, and Fe, in some market milk samples. The heavy metals concentrations were lower than the Egyptian Standard of Food 7136 and WHO standard and did not exceed the permissible limits.

3.2. Measurements of the open circuit potential

The potential-time change of the four electrodes in milk and tap water at 30°C is shown in Figure 1. The potential of CoCr-alloy, Mo, and Nb electrodes in milk shifted over time in a positive direction before stabilizing with longer immersion times. This denotes the development of an oxide film that gives the electrodes passivity [20]. The potential of the Au electrode, on the other hand, changed to negative values and stabilized when immersion time was increased. The same behavior was seen for all investigated electrodes at 20, 40, and 50°C. The potentials of the CoCr-alloy, Au, and Nb electrodes shifted in the positive direction in tap water, while the potentials of the Mo electrode shifted in the negative direction.

The passivation of the Nb and CoCr-alloy electrodes was evidenced by a shift in their potential towards a positive direction in both milk and tap water. This behavior was explained for the Nb electrode by its extremely high reactivity with water, which, in accordance with reaction (1), results in the production of a protective pentoxide film. The lowest energy state for Nb atoms is represented by a niobium ion in the pentoxide. [21].

$$2\mathrm{Nb} + 5\mathrm{H_2O} \rightarrow \mathrm{Nb_2O_5} + 10\mathrm{H^+} + 10\ \mathrm{e^-}$$
$$\mathrm{E^\circ} = -0.644\ \mathrm{V} \qquad (1)$$

In the case of the CoCr-alloy electrode, the passivity was brought on by the development of a thermodynamically stable passive oxide film ($\mathrm{Cr_2O_3}$) rich in chromium at the electrode surface. Here, metal in a passive state will still corrode uniformly and slowly, but it will not dissolve quickly as would otherwise happen due to thermodynamic forces [22]. When chromium metal is present in the air, it spontaneously forms $\mathrm{Cr_2O_3}$ at the electrode surface, as shown by reaction (2) [23]. Figure 1 shows that CoCr- alloy in the two tested solutions had greater potential than an Au electrode twenty minutes into the experience. The biocompatibility of CoCr- alloy is closely linked to its high resistance to corrosion, which is attributed to the spontaneous formation of a passive oxide film.

$$2Cr + 3H_2O \rightarrow Cr_2O_3 + 6H^+ + 6e^-$$
$$\mathrm{E^\circ} = -0.9927\ \mathrm{V} \qquad (2)$$

The increase in the potential of the Mo electrode at the onset of immersion in milk coincides with the creation of trioxide film covering the electrode surface according to reaction (3). It was suggested that $\mathrm{Mo_2O_3}$ developed along the metal/film interface during the early stages of passivation [24]

$$2\mathrm{Mo} + 3\mathrm{H_2O} \rightarrow \mathrm{Mo_2O_3} + 6\mathrm{H^+} + 6\mathrm{e^-} \qquad (3)$$

The comparatively constant potential of gold in tap water is evidence to its well-known resistance to oxidation and corrosion. This behavior was interpretable according to the Pourbaix diagram, which shows that the metal is most stable in neutral to slightly basic conditions and exists largely as metallic gold. This indicates that the metal is stable and doesn't undergo any notable oxidation or reduction processes under typical circumstances [2].

The creation of a protective oxide covering on the electrode surface coincides with potential shifts toward positive values. The following equation can be used to represent the relationship between potential and time for electrodes loaded with skinny films:

$$|\mathrm{E}| = \text{ḍ} + 2.303\ (\delta/\beta)\ \log t \qquad (4)$$

Where (|E|) is the electrode potential, ḍ is the thickness of the skinny film and δ represents the rate of oxide thickening per unit decade of time. The term β is identified as:

$$\beta = \frac{nF}{RT}\ \alpha\ \delta` \qquad (5)$$

Where n is the number of electrons transferred in the reaction, F is Faraday's constant, R is the universal gas constant, T is the absolute temperature, α is the

charge transference coefficient encountered in normal electrochemical processes ($0 < \alpha < 1$) and δ` is the height of the energy barrier surmounted during charge transfer [20]. Figure 2 shows a graphic representation of Equation 4 by graphing the electrode potential against the logarithm of time. Tables 4 and 5 contain the rates of oxide thickening as computed from the slopes of the straight lines.

Table 1: Results of tap water analysis in mg/L for three different samples taken in the same day

	Type of analysis	Sample 1	Sample 2	Sample 3	Available range
Physical analysis	Color	-	-	-	-
	Taste	Accepted	Accepted	Accepted	Accepted
	Odor	-	-	-	-
	Free residual chlorine	-	-	-	5
	Turbidity N.T.U	3	0.6	1.0	1
	pH	7	6.5	7.8	6.5 : 8.5
	Electrical conductivity Us/cm	365	350	381	-
Chemical analysis	NH_3	0.2 >	0.2 >	0.2 >	0.5
	NO_2	-	-	0.07	0.2
	NO_3	1.3	1 >	1 >	45
	Cl	20	30	24.5	250
	F	0.3 >	0.3 >	0.3 >	0.8
	SO_4	35	32	12.7	250
	Na	34	25.2	31	200
	K	5	5.16	3.1	-
	Ca	29.6	36.8	30.8	-
	Mg	8.64	6.72	9.84	-
	Fe	-	-	-	0.3
	Mn	-	-	-	0.4
	SiO_2	3	6	20	-
	Total hardness $CaCO_3$	110	120	118	500
	Temporary hardness $CaCO_3$	110	100	118	-
	Permanent hardness $CaCO_3$	-	20	-	-
	Calcium hardness $CaCO_3$	74	92	77	350
	Magnesium hardness $CaCO_3$	36	28	41	150
	Total alkalinity $CaCO_3$	122	100	140	-
	Hydroxide alkalinity $CaCO_3$	-	-	-	-
	Carbonate alkalinity $CaCO_3$	-	-	-	-
	Bicarbonate alkalinity $CaCO_3$	122	100	140	-
	Total dissolved salts T.D.S	215	215	226	1000
	HCO_3	148.84	122	170.8	-
Heavy metal analysis	Mo	0.003	-	0.009	0.07
	Zn	0.019	0.003	0.0002	3.0
	Pb	-	0.0004	0.0002	0.01
	Cd	-	-		0.003
	Cr	0.0003	-	0.002	0.05
	Al	0.0020	0.004		0.2
	Cu	0.0086	0.002	0.0002	2.0
	Ba	0.005	0.008	0.079	0.7
	Ni	-	-	0.0007	0.02
	Se	-	-	-	0.01
	Sb	-	-	-	0.02
	Hg	0.0004	-	-	0.001

	As	-	-	-	0.01

Table 2: Results of tap water analysis in mg/L for three different samples taken among three months

Type of analysis		Sample 1	Sample 2	Sample 3	Available range
Physical analysis	Color	-	-	-	-
	Taste	Accepted	Accepted	Accepted	Accepted
	Odor	-	-	-	-
	Free residual chlorine	0.5	1.1	2	5
	Turbidity in N.T.U	1.0	1.0	1.0	≤ 1
	pH	8.1	7.5	7.8	6.5:8.5
	Electrical conductivity Us/cm	402	431	359	-
Chemical analysis	NH_3	-	-	-	0.5
	NO_2	-	-	-	0.2
	NO_3	-	-	-	45
	T.D.S /120 mL	265	284	237	1000
	Cl	38	41	32	250
	SO_4	35	38	36	250
	Na	42	45	28	200
	Mn	-	-	-	0.4
	Fe	-	-	-	0.3
	F	0.2	0.2	0.2	0.8
	Calcium hardness $CaCO_3$	90	97	81	350
	Magnesium hardness $CaCO_3$	46	50	42	150
	Total hardness $CaCO_3$	136	147	123	500
	Total alkalinity $CaCO_3$	123	132	105	-

Table 3: Results of milk analysis in mg/L for three different samples

	Type of analysis	Sample 1	Sample 2	Sample 3	Reference range
1	Total fat	3.00	3.1	3.0	not less than 3%
2	Total solids	11.6	11.9	11.4	not less than 11.3 %
3	Solids not fat	8.3	8.8	8.4	not less than 8.25 %
4	formalin	-	-	-	-
5	Acidity as lactic acid	0.12	0.12	0.12	up to 0.17 %
6	Benzoic acid and it's salt	-	-	-	-
7	Sorbic acid and it's salt	-	-	-	-
8	Sulfur dioxide and it's salt	-	-	-	-
9	Lead	-	-	-	less than 20 ppd
10	Toxicological fungous	-	-	-	-
11	Pesticide	< 0.01	< 0.01	< 0.01	LOQ = 0.01 mg/Kg

Tables 4 and 5 show how temperature has an impact on the stable potentials. Steady-state potential, E_{ss}, dropped in the four electrodes in tap water (Table 5) at all temperatures as follows: CoCr- alloy > Au > Mo > Nb. Milk at 20, 30, and 40°C behave similarly (Table 4), while at 50°C its behavior changed to follow the following order: Au > CoCr- alloy > Mo > Nb.

E_{ss} values for each electrode fell as the temperature rose. One exception was a Mo electrode in milk solution that was recorded at 30°C and had a constant potential that was lower than those recorded at 40 and 50°C. Tables 4 and 5 further showed that all investigated electrodes have larger stable potentials in tap water than in milk solutions at all temperatures. More passivation in tap water is indicated by this observation. Positive slopes of E *vs.* log t plots signify the thickening of the film. The dissolution of the electrodes was guaranteed by the negative slopes for the Au electrode in milk and the Mo electrode in tap water.

3.3. Measurements of the potentiodynamic polarization

The polarization plots for the four electrodes in milk and tap water, at 30°C, are shown in Figures 3 and 4 respectively. The optimal behavior of Tafel plots is shown by the polarization curves of the Au and Mo electrodes. The polarization curves of the two tested solutions showed a passivity range for CoCr- alloy following the initial anodic dissolution region. This denotes the development of a less stable passive film, which contains non-stoichiometric cobalt oxides and certain oxides of alloying elements [25]. With tap water, this tendency was more observable. Normally Tafel plots are measured within a potential window from + 250 to - 250 mV around the OCP, and Tafel slopes are

deduced within this range. The detected abnormal behavior of the niobium electrode was the main reason behind the extended potential window of Tafel measurements. Under conditions of high potentials, the niobium electrode curves in the two tested solutions revealed low current density *vs.* potential at the anodic region, forming large current density plateaus that ensure considerable corrosion resistance. In prior work, similar behavior of Nb in artificial saliva and fluoride solutions was demonstrated [26, 27].

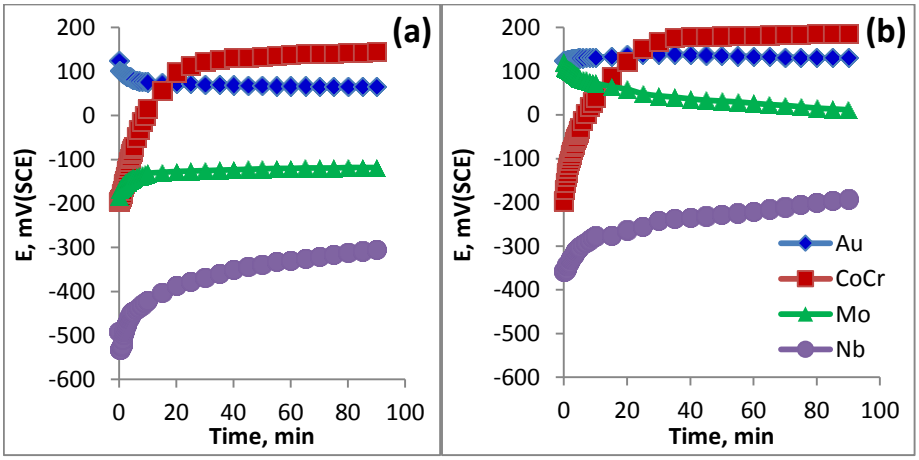

Figure 1: Potential – time plots of the studied electrodes in milk (a) and water (b) at 30 °C.

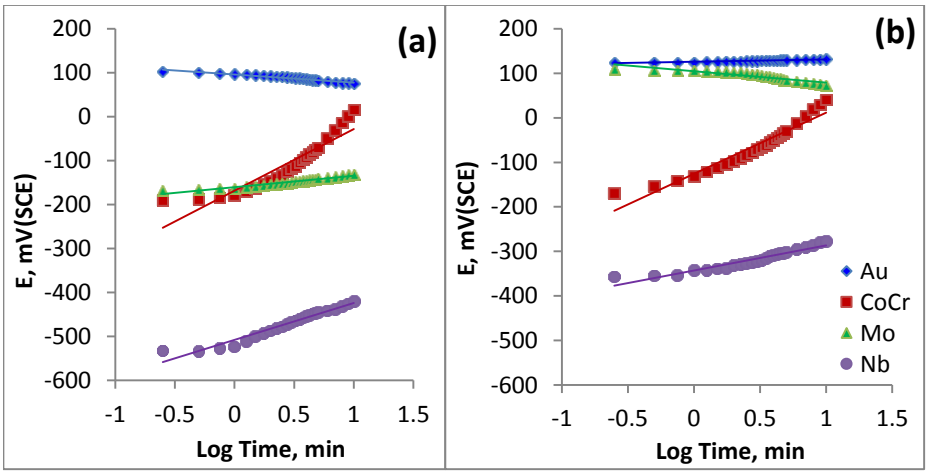

Figure 2: E –Log t plots of the tested electrodes in milk (a) and tap water (b) at 30°C.

A helpful method to determine the corrosion current densities (I_{corr}) and, subsequently, the corrosion rates in similar situations was to extrapolate the cathodic polarization curves alone to E_{corr}. Using Eq. 6 [27], the corrosion rate (C_R) in mpy was computed.

$$C_R = 0.13 \times I_{corr} \times e/d \qquad (6)$$

where 0.13 is the metric and time conversion factor, I_{corr}, is the corrosion current density in μA/cm², e and d are the equivalent weight and density of metal in geq/mol and g/cm^3 respectively.

The corrosion potential (E_{corr}) and corrosion current density (I_{corr}) values were computed from the intersection of the linear anodic and cathodic branches of the Tafel plots. Tables 6-9 list each of these variables as well as the anodic (β_a) and cathodic (β_c) Tafel slopes for the various electrodes.

The analysis of the data in Tables 6- 9 demonstrated that, for all analyzed electrodes, the corrosion rates (C_R) increased with rising temperature in each milk and tap water. The results illustrated that milk corroded the four electrodes more quickly than tap water did at all experimental temperatures. The highest corrosion rate values for all electrodes were provided by the Nb electrode in milk. Following are the passivity orders consistent with corrosion rate values:

In milk: Au > Mo > CoCr- alloy > Nb

In water: Au > Mo > Nb > CoCr- alloy

Table 4: Immersion (E_{imm}) and steady state (E_{ss}) potentials, slopes of the linear parts, rates of the oxide film thickening (δ), and regression coefficient (R^2) of the tested electrodes in milk, at temperature ranges 20 – 50°C

Type of electrode	Temp. °C	E_{imm} mV(SCE)	E_{ss} mV(SCE)	Slope mV/min.	δ nm/min	R^2
Au	20	143	76	-24.35	-	0.9687
	30	125	66	-12.86	-	0.9476
	40	112	58	-11.61	-	0.9476
	50	99	51	-5.57	-	0.9473
CoCr	20	-120	183	45.51	1174	0.8505
	30	-196	145	97.47	2432	0.8566
	40	-205	74	100.31	2423	0.8748
	50	-280	-64	65.43	1736	0.9740
Mo	20	-151	-84	8.83	456	0.9567
	30	-185	-118	25.23	1259	0.9410
	40	-231	-107	21.00	1014	0.8668
	50	-255	-129	15.73	737	0.8232
Nb	20	-427	-291	63.27	5442	0.7374
	30	-490	-304	83.98	6984	0.9529
	40	-500	-310	67.80	5008	0.9275
	50	-500	-322	85.62	6680	0.9021

Table 5: Immersion (E_{imm}) and steady state (E_{ss}) potentials, slopes of the linear parts, rates of the oxide film thickening (δ) and regression coefficient (R^2) of the tested electrodes in tap water, at temperature ranges 20 – 50°C

Type of electrode	Temp. °C	E_{imm} mV(SCE)	E_{ss} mV(SCE)	Slope mV/min.	δ nm/min	R^2
Au	20	129	136	1.30	34	0.7390
	30	125	131	5.13	128	0.9037
	40	113	126	11.64	281	0.7989
	50	109	124	13.25	310	0.7060
CoCr	20	-165	212	67.40	1739	0.9579
	30	-197	186	81.50	2033	0.9739
	40	-237	183	90.13	2177	0.9624
	50	-263	179	90.26	2112	0.9553
Mo	20	159	80	-9.77	-	0.9422
	30	121	12	-11.21	-	0.8838
	40	30	-63	-23.66	-	0.9755
	50	14	-85	-17.33	-	0.8522
Nb	20	-346	-190	46.95	4038	0.8565
	30	-357	-192	56.45	4695	0.9208
	40	-380	-210	13.14	1058	0.8564
	50	-398	-248	57.73	4504	0.9055

This order was observed at temperatures between 20 and 50 °C, indicating that in the case of tap water and milk, under potentiodynamic circumstances, Mo could safely replace Au at all investigated temperatures. Artificial saliva solution, in a previous study, showed the same behavior [26].

During the 1920s, a correlation between rising milk temperature and increased electrode dissolving rates was found. The concurrent growth in the bacteria that produce lactic acid was the primary cause of this behavior. In other words, milk's acidity rises and its oxygen concentration falls when the temperature rises [28, 29].

The data also demonstrate that tap water was the least corrosive to all tested electrodes when compared to milk and other previously examined neutral solutions at temperatures between 20 and 50 °C [26, 27]. As the temperature rises and the electrode is connected to the tested solution for longer periods, the media's color becomes more intense, signaling the occurrence of various chemical reactions as well as other processes like fermentation, oxidation, and the dissolution of corrosion products.

The data of open circuit potential and potentiodynamic polarization ensured that milk is more corrosive than tap water for the four tested electrodes. This may be due to the Protein content in milk. Hamad and Baiomy [30] stated that the percentage of protein in milk represents 3.37%. While cobalt and chromium are

positively charged ions, the majority of proteins are negatively charged. The protein is thus readily adsorbed to the metal alloy surface. For both high and low-carbon CoCr-alloys, Yan et al. [31, 32] reported that the proteins can improve ion release and passive film disintegration under static corrosion conditions. This happened when the passive zone was reduced as a result of proteins adhering to the alloy surface.

The Tafel slope assumes that the electrode surface is uniform and homogeneous. However, surface roughness, impurities, or defects on the electrode surface can affect the reaction kinetics and result in anomalous Tafel slope values as shown in Tables 6-9. Attia and coworkers in a previous study of the corrosion protection of Tin in 1M HCl attributed the high values of Tafel slopes to the surface kinetic process instead of diffusion controlled process [33]. Another interpretation of the high Tafel slope values in this work is based on the fact that the Tafel slope is a measure of the rate at which the current changes with the applied potential in an electrochemical reaction. These electrochemical reactions often involve the adsorption and desorption of reactants or intermediates on the electrode surface. If these adsorption/desorption processes deviate from the normal mode, anomalous Tafel slope values may be obtained. Also, the formation of intermediate species can affect the reaction rate and consequently affect the Tafel slope values.

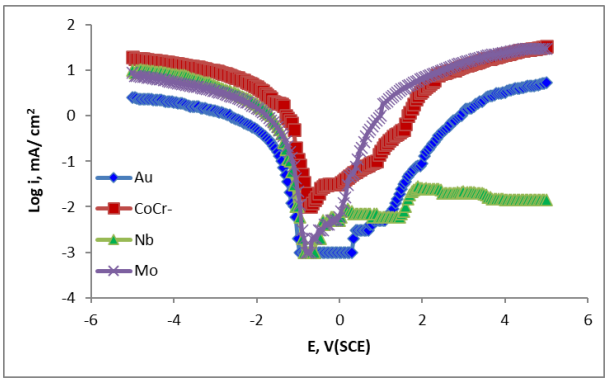

Figure 3: Potentiodynamic plot of CoCr-alloy, Nb, Mo, and Au electrodes in milk at 30°C.

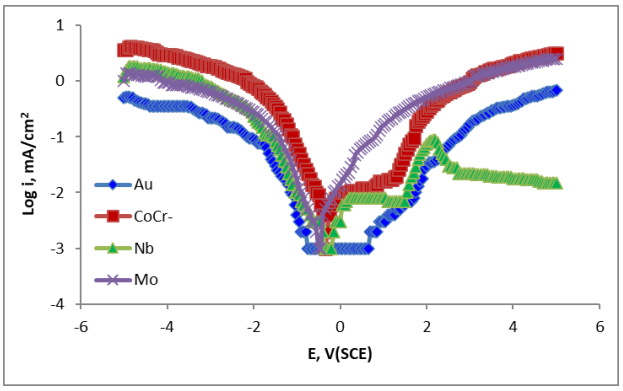

Figure 4: Potentiodynamic plot of CoCr-alloy, Nb, Mo, and Au electrodes in tap water at 30°C.

According to the theory, an electrode that is more likely to passivate will have a value of $\beta_a > \beta_c$, whereas an electrode that is more likely to corrode will have a value of $\beta_a < \beta_c$ [34]. A general tendency in this investigation showed larger values of β_a in contrast to β_c, which points to an inactive layer being present on the electrode surface.

3.4. Kinetic and Thermodynamic considerations

The following Arrhenius equation relates the corrosion rate (C_R) with the variation of temperature [27]:

$$\log C_R = A - (E_a/2.303\,RT) \qquad (7)$$

where A is constant represents the frequency factor of successful collisions between reactant molecules. E_a is the apparent activation energy of the dissolution reaction, R is the universal gas constant and T is the absolute temperature. Straight lines with a slope of $-(E_a/2.303\,R)$ were produced by plotting the logarithmic fluctuation of corrosion rates with the reciprocal of absolute temperatures as illustrated in Figures 5 and 6. Table 10 contains records of the obtained values.

Table 6: Milk and tap water potentiodynamic parameters for Au electrode

Neutral solution	Temp. °C	E_{corr} mV/SCE	I_{corr} µA/cm²	β_c mV/dec	β_a mV/dec	C_R mpy
Milk	20	100	0.0316	-1833	1800	3.24 E-06
	30	-100	0.0398	-1750	1750	4.08 E-06
	40	-100	0.0501	-1600	1750	5.14 E-06
	50	-100	0.0631	-1400	2000	6.47 E-06
Tap water	20	400	0.0126	-899	2500	1.29 E-06
	30	200	0.0200	-3000	2500	2.05 E-06
	40	200	0.0251	-3000	3000	2.58 E-06
	50	100	0.0316	-2000	2000	3.24 E-06

Table 7: Milk and tap water potentiodynamic parameters for CoCr- alloy electrode

Neutral	Temp.	E_{corr}	I_{corr}	β_c	β_a	C_R

solution	°C	mV/SCE	μA/cm²	mV/dec	mV/dec	mpy
Milk	20	-200	0.501	-2000	2000	1.54 E-01
	30	-200	0.631	-2000	2000	1.94 E-01
	40	-200	0.794	-1667	2333	2.44 E-01
	50	-200	0.891	-1250	2000	2.74 E-01
Tap water	20	100	0.039	-1750	2000	1.22 E-02
	30	-100	0.079	-2000	2333	2.44 E-02
	40	-100	0.100	-1400	1333	3.08 E-02
	50	-100	0.199	-1750	1667	6.14 E-02

Table 8: Milk and tap water potentiodynamic parameters for Mo electrode

Neutral solution	Temp °C	E_{corr} mV/SCE	I_{corr} μA/cm²	β_c mV/dec	β_a mV/dec	C_R mpy
Milk	20	-300	0.040	-1000	875	8.05 E-03
	30	-500	0.063	-1125	1000	1.27 E-02
	40	-600	0.100	-1000	1333	2.02 E-02
	50	-700	0.199	-1500	1428	4.04 E-02
Tap water	20	-400	0.012	-1200	1333	2.55 E-03
	30	-500	0.025	-1400	1750	5.08 E-03
	40	-600	0.040	-1000	2000	8.05 E-03
	50	-600	0.050	-1600	2333	1.01 E-02

Positive values of constant (A) recorded for CoCr-alloy, Mo and Nb electrodes mean that the dissolution reaction is relatively fast, and it does not require a high activation energy to proceed. On the contrary, the negative value of A recorded for the Au electrode implies that the reaction has a lower frequency of successful collisions, meaning that the reaction is less likely to occur. Negative activation energy values (E_a) for the corrosion process of electrodes indicate that the process is exothermic and spontaneous. This means that the reaction occurs readily and quickly, without a significant energy barrier. This could be due to the nature of the metal/solution interaction, which could be highly favorable and spontaneous.

Table 10 shows that whereas CoCr- alloy dissolves rather slowly in milk solution, Nb passive film dissolves quickly. This conclusion was drawn from the numerical values of activation energy, where the CoCr-alloy electrode supplied the least negative value and the Nb electrode the largest negative value in the milk solution. The largest negative E_a value in tap water was produced by CoCr- alloy, whereas the Au electrode gave the value with the least negative sign. Less negative E_a values in one medium suggested that the corrosion reaction's energy barrier was higher in that medium due to its increased height.

The thermodynamic functions for the dissolution process were obtained by applying the Eyring transition-state equation (Eq. 8) [26]:

$$\log C_R/T = \log (R/Nh) + (\Delta S^{\circ}/2.303R) - (\Delta H^{\circ}/2.303RT) \quad (8)$$

where Avogadro's number is N, Planck's constant is h, and the entropy and enthalpy changes of activation, respectively, are ΔS° and ΔH°. As shown in Figures (7 and 8), straight lines with slopes of $[-\Delta H^{\circ}/2.303R]$ and an intercepts of $[\log(R/Nh) + (\Delta S^{\circ}/2.303R)]$ were obtained from a plot of $\log C_R/T$ vs. $1/T$. The results were compiled in Table 11.

When a metal corrodes, the metal atoms or ions break apart from the solid lattice and interact with the solvent molecules. This process requires energy input to overcome the attractive forces holding the metal together and to separate the metal particles. The positive enthalpy change (ΔH°) for all electrodes, reflects the endothermic character of the corrosion process where the system gains energy from the surroundings. This suggested that the electrodes would dissolve slowly and with difficulty in the presence of existing conditions, indicating a higher level of protection [35]. The high ΔH° values might be attributable to the adsorption of the solutions to the electrode surfaces, which increased the enthalpy of the corrosion process [36]. There is no contrast in data submitted from Tables 10 and 11 concerned with negative activation energy and positive enthalpy change for the tested electrodes. However, a dissolution reaction of an electrode could have a positive enthalpy if the energy required for breaking the metal/solute and solvent/solvent interactions is greater than the energy released by the formation of new metal/solvent interactions. At the same time, a dissolution reaction could have negative activation energy when the reaction occurs readily and quickly due to a highly favorable reaction.

Additionally, all electrodes had substantial and uniformly negative entropy change values (ΔS°). This indi-

cates that the metal ions become more organized during the corrosion process. This could happen, if the metal ions form clusters in the solution, leading to a decrease in randomness.

Therefore, it was established that factors such as the nature, composition, pH, and temperature of the solution, as well as the type of electrode, activation energy, enthalpy, and entropy changes, had a significant impact on the activation parameters of the corrosion process to occur.

Table 9: Milk and tap water potentiodynamic parameters for Nb electrode

Neutral solution	Temp. °C	E_{corr} mV/SCE	I_{corr} µA/cm^2	β_c mV/dec	β_a mV/dec	C_R mpy
Milk	20	-700	1.259	-4000	-	1.78 E-01
	30	-800	1.585	-4500	-	2.24 E-01
	40	-800	1.995	-7000	-	2.81 E-01
	50	-800	3.162	-5500	-	4.46 E-01
Tap water	20	100	0.050	-4000	-	7.07 E-03
	30	-300	0.063	-2667	-	8.90 E-03
	40	-400	0.126	-2333	-	1.78 E-02
	50	-400	0.200	-4500	-	2.82 E-02

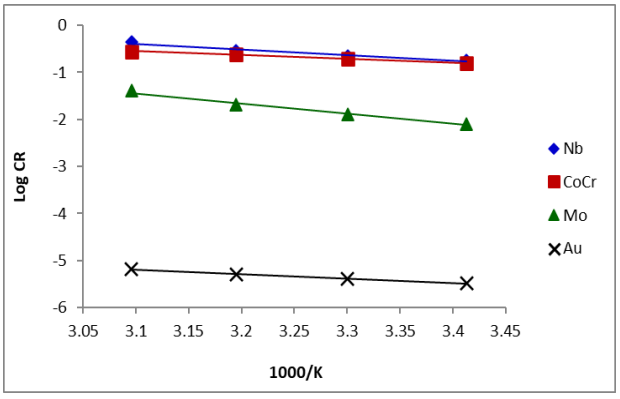

Figure 5: Arrhenius plot of the milk-dipped electrodes under investigation

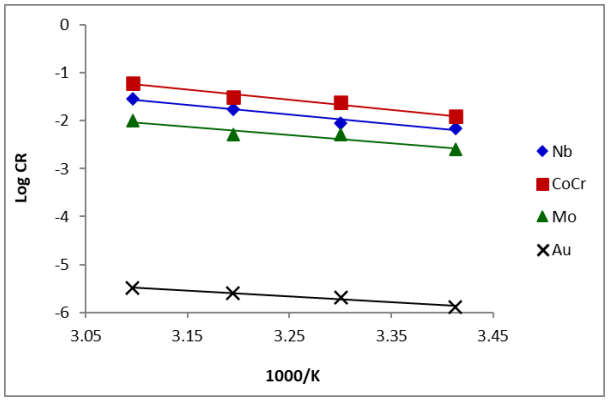

Figure 6: Arrhenius plot of the tap water-dipped electrodes under investigation.

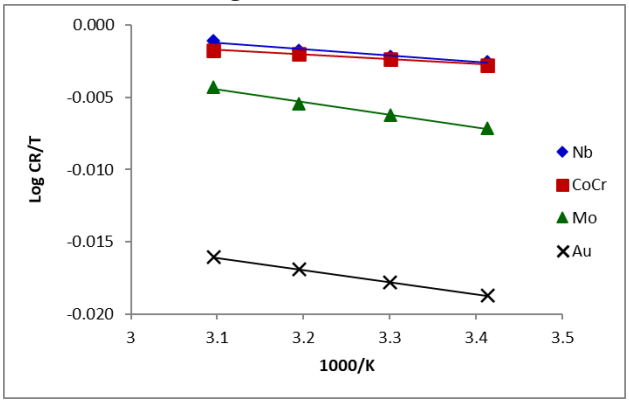

Figure 7: Transition state graph showing the corrosion behavior of the investigated electrodes in milk.

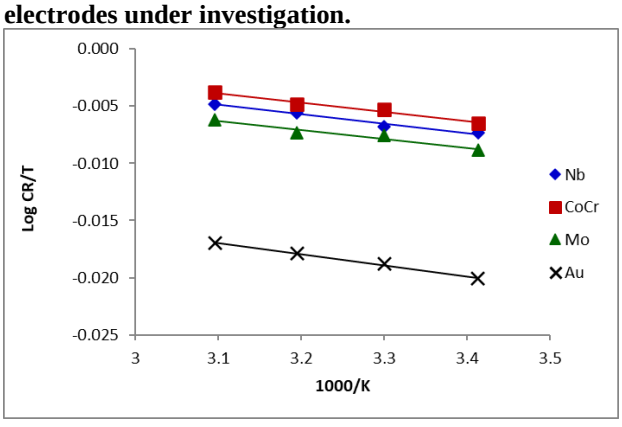

Figure 8: Transition state graph showing the corrosion behavior of the investigated electrodes in tap water.

Table 10: Milk and tap water activation parameters for the investigated electrodes

Type of Electrode	Milk			Tap water		
	A	E_a, kJ/mol	R^2	A	E_a, kJ/mol	R^2
CoCr	1.9	-15	0.989	5.204	-40	0.967
Au	-2.3	-18	0.999	-1.652	-23	0.973
Mo	5.3	-41	0.982	3.237	-33	0.899
Nb	3.4	-65	0.955	4.573	-24	0.962

Table 11: Milk and tap water thermodynamic parameters for the investigated electrodes

Type of Electrode	Milk			Tap water		
	ΔS° J/mol K	ΔH° KJ/mol	R^2	ΔS° J/mol K	ΔH° KJ/mol	R^2
CoCr	-197	63	0.989	-197	160	0.978
Au	-197	161	1.000	-197	186	0.993
Mo	-197	169	0.993	-197	150	0.947
Nb	-197	87	0.974	-197	159	0.980

4. Conclusions

1. Measurements of the open circuit potential showed that the CoCr-alloy, Mo, and Nb electrodes in milk solution have developed passive oxide layers.
2. In tap water, passive oxide layers were formed on CoCr- alloy, Au, and Nb electrodes. After the first 20 minutes of immersion, CoCr- alloy in milk and tap water exhibits greater potential values than Au electrode.
3. According to polarization measurements, the corrosion rates of all electrodes increased as temperature rose, and the following orders represent the sequence of passivity:
   In milk: Au > Mo > CoCr-alloy > Nb
   In tap water: Au > Mo > Nb > CoCr-alloy
4. At all tested temperatures in tap water and milk, Au may be safely replaced by Mo under potentiodynamic conditions.
5. The apparent activation energy of the dissolution reaction (E_a) indicates that the Nb passive film dissolves readily in milk whereas the CoCr-alloy dissolves somewhat slowly.
6. The easiest electrode to dissolve in tap water is CoCr- alloy, whereas Au is more challenging.

References

1. J. O. Listopad, K. Sarna-Bos, A. Szabelska, E. C. Piszcz, J. Borowicz, J. Szymanska, The use of gold and gold alloys in prosthetic dentistry – a literature review. Curr. Issues Pharm. Med. Sci. 28(3) (2015)192-195. DOI:10.1515/cipms-2015-0070
2. M. Pourbaix, Atlas of electrochemical equilibria in aqueous solutions. (NACE International, Houston, TX, 1974).
3. P. Bleckenwegner, C. C. Mardare, C. Cobet, J. P. Kollender, A. W. Hassel, A. I. Mardare, compositionally dependent nonlinear optical band gap behavior of mixed anodic oxides in niobium-titanium system. ACS Comb. Sci. 19(2) (2017) 121-9.
4. S. Nasibia, K. Alimohammadib, L. Bazlic, S. Eskandarinezhadd, A. Mohammadie, N. Sheysie, TZNT alloy for surgical implant applications: A Systematic Review. J. Compos. Compou. 2 (2020) 61-67. DOI:10.29252/jcc.2.2.1
5. S. Acharya, A.G. Panicker, D.V. Laxmi, S. Suwas, K. Chatterjee, Study of the influence of Zr on the mechanical properties and functional response of Ti-Nb-Ta- Zr-O alloy for orthopedic applications. Mat. Des. 164 (2019) 107555. DOI: 10.1016/j.matdes.2018.107555
6. S. Acharya, A.G. Panicker, V. Gopal, S.S. Dabas, G. Manivasagam, S. Suwas, K. Chatterjee, Surface mechanical attrition treatment of low modulus Ti-Nb- Ta-O alloy for orthopedic applications. Mat. Sci. Eng.: C 110: (2020) 110729.
7. J. D. M. Matos, A. C. M. Dos Santos, L. J. N. Nakano, J. E. L. De Vasconcelos, V. C. Andrade, R. S. Nishioka, M. A. Bottino, G. R. S. Lopes. Metal alloys in dentistry: an outdated material or required for oral rehabilitation? Int. J. Odontostomat. 15(3) (2021) 702-711. DOI:10.4067/S0718-381X2021000300702
8. S. F. Jawed, C.D. Rabadia, Y. Liu, L.Q. Wang, P. Qin, Y.H. Li, X. Zhang, L.C. Zhang, Strengthening mechanism and corrosion resistance of beta-type Ti-Nb-Zr-Mn alloys. Mat. Sci. Eng. C 110: (2020) 110728. DOI: 10.1016/j.msec.2020.110728
9. U. R. Evans, The corrosion and oxidation of metals 2nd supplementary volume, pp. 162. (1976).
10. E. M. Attia, Effect of two triazole thione derivatives on corrosion behavior of molybdenum in 0.01MHCl. Al-Azhar Bull. Sci. 19(1) (2008) 135-151.
11. E. M. Attia, A. E. EL- Shennawy, W. A. M. Hussein, Electrochemical behavior of molybdenum electrode in acetic, formic and oxalic acid solutions. Al-Azhar Bull. Sci. 19(1) (2008) 27-39.
12. M. S. Jasinska, L. M. Morath, M. P. Kwesiga, M. E. Plank, A. L. Nelson, A. A. Oliver, M. L. Bocks, R. J. Guillory II, J. Goldman. In-vivo evaluation of molybdenum as bioabsorbable stent candidate. Bioact. Mat. 14 (2022) 262–271. DOI: 10.1016/j.bioactmat.2021.11.005
13. S. J. Sadowsky, Has zirconia made a material difference in implant prosthodontics? A review. Dent. Mater. 36(1) (2020) 1-8. DOI: 10.1016/j.dental.2019.08.100
14. Y. S. Al Jabbari, Physico-mechanical properties and prosthodontic applications of Co-Cr dental alloys: a review of the literature. Adv. Prosthodont. 6 (2) (2014) 138-145. DOI:10.4047/jap.2014.6.2.138
15. F. Mayinger, D. Micovic, A. Schleich, M. Roos, M. Eichberger, B. Stawarczyk, Retention force of polyetheretherketone and cobalt-chrome-molybdenum removable dental prosthesis clasps after artificial aging. Clinical Oral Investigations. 25 (2021) 3141–3149. DOI:10.1007/s00784-020-03642-5
16. X. Xing, Q. Hu, Y. Liu, Y. Wang, H. Cheng, Comparative analysis of the surface properties and corrosion resistance of Co-Cr dental alloys fabri-

cated by different methods. J. Prosthet. Dent. 5; S0022-3913(21)00652-1. (2022). Doi: 10.1016/j.prosdent. 2021.11.019.
17. P. F. Fox, T. Uniacke-Lowe, P. L. H. McSweeney, J.A. O'Mahony, Dairy Chemistry and Biochemistry. (2015) 241-270. DOI:10.1007/978-3-319-14892-2
18. A. A. Eleboudy, A.A. Amer, H.S. Abo El-Makarem, H. H. Abo Hadour, Heavy metals residues in some dairy products. AJVS. 52(1) (2017) 334-346. DOI: 10.5455/ajvs.230723
19. A. E. Mohamed, M. N. Rashed, M. M. Aboelhassn, Determination of heavy metals in preserved milk using microwave digestion and atomic absorption spectroscopy. AUJES. 2(4) (2021) 290-301. DOI: 10.21608/aujes.2021.99317.1044
20. F.E. Heakal, A.A. Ghoneim, A.M. Fekry, Stability of spontaneous passive films on high strength Mo-containing stainless steels in aqueous solutions. J. Appl. Electrochem. 37 (2007) 405–413. DOI:10.1007/s10800-006-9271-3
21. R. E. Ricker, G. R. Myneni, Evaluation of the propensity of niobium to absorb hydrogen during fabrication of superconducting radio frequency cavities for particle accelerators. J. Res. Natl. Inst. Stand. Technol. 115 (5) (2010) 353-371.
22. G. Bellefontaine, The corrosion of CoCrMo alloys for biomedical applications. School of Metallurgy and Materials, M.Sc. University of Birmingham. Birmingham. (2010)1-88.
23. N. Kovačević, B. Pihlar, V.S. Selih, I. Milošev, The effect of pH value of a simulated physiological solution on the corrosion resistance of orthopaedic alloys. Acta Chim. Slovenica. 59(1) (2012) 144-155.
24. V. S. Saji, C-W Lee, Molybdenum, molybdenum oxides, and their electrochemistry. ChemSusChem, 5(7) (2012) 1146 – 1161. DOI: 10.1002/cssc.201100660
25. I. V. Branzoi, M. Iordoc, M. M. Codescu, Corrosion behaviour of CoCrMo and CoCrTi alloys in simulated body fluids. U.P.B. Sci. Bull. Series B, 69(4) (2007) 11– 18.
26. E. M. Attia, R.M. Abou Shahba, F.M. Abou Koffa, Open circuit potential and potentiodynamic view on the behavior of different four electrodes in artificial saliva solution for usage in dental application. J. Basic. Appl. Chem. 8(3) (2018) 9-18.
27. E. M. Attia, R.M. Abou Shahba, F.M. Abou Koffa, Electrochemical behavior of Nb and Mo electrodes compared with CoCr-alloy and Au electrodes in fluoride solutions for dental application. J. Basic. Appl. Chem. 9(1) (2019) 1-7.
28. E. W. Schultz, M. Albert, I. J. Beaver, The Relationship between the hydrogen ion concentration and the bacterial content of commercial milk. J. Dairy Science 4 (1) (1921) 1-6.
29. E. Duncombe, The influence of certain factors on the hydrogen ion concentration of milk. II. Temperature Changes. J. Dairy Science 7(3) (1924) 245-248.
30. M. N. E. Hamad, A. A Baiomy, Physical properties and chemical composition of cow's and buffalo's milk in Qena governorate. J. Food and Dairy Sci. 1(7) (2010) 397- 403. DOI:10.21608/jfds.2010.82466
31. Y. Yan, A. Neville, D. Dowson, Biotribocorrosion - an appraisal of the time dependence of wear and corrosion interactions: II. Surface analysis. J. Phys. D-App. Phys. 39(15) (2006) 3206-3212. DOI:10.1088/0022-3727/39/15/S11
32. Y. Yan, A. Neville, D. Blowson. Biotribocorrosion of CoCrMo orthopaedic implant materials - Assessing the formation and effect of the biofilm. Tribology Int. 40(10-12) (2007) 1492-1499. DOI: 10.1016/j.triboint.2007.02.019
33. E. M. Attia, N. S. Hassan, A. M. Hyba, Corrosion Protection of Tin in 1M HCl by expired primperan and E-mox drugs-Part I. J. Basic. Appl. Chem. 7(1) (2017) 9-25.
34. E. M. Attia, O. E. Elazabawy, N. S. Hassan, A. M. Hyba, Potentiodynamic study on the corrosion inhibition of carbon steel in formation water by potato peel extract. IJARP. 4(3) (2020) 79-84.
35. E.M. Attia, Dipron: an eco-friendly corrosion inhibitor for iron in HCl media in both micro and nano scale particle size - Comparative study. IJARP. 4(3) (2016) 986-1003.
36. E. M. Attia, N. S. Hassan, A. M. Hyba, corrosion protection of tin in 1M HCl by expired Novacid drug-Part I. IJAR. 4(2) (2016) 872-886.